

Short-Lived Electron Transfer in Donor-Bridge-Acceptor Systems

D. Psiachos^{a,*}

^a*Department of Physics, University of Crete, Heraklion 71003, Greece*

Abstract

We investigate time-dependent electron transfer (ET) in benchmark donor-bridge-acceptor systems. For the small bridge sizes studied, we obtain results far different from the perturbation theory which underlies scattering-based approaches, notably a lack of destructive interference in the ET for certain arrangements of bridge molecules. We also calculate wavepacket transmission in the non-steady-state regime, finding a featureless spectrum, while for the current we find two types of transmission: sequential and direct, where in the latter, the current transmission *increases* as a function of the energy of the transferred electron, a regime inaccessible by conventional scattering theory.

Keywords: tunnelling, electron transfer, quantum wires, non-perturbative methods

1. Introduction

Electron transfer (ET) in donor-bridge-acceptor (D-B-A) systems composed of organic molecules or molecular chains has been studied actively for the past few decades due to the potential applications to molecular electronics, DNA, etc. Expressions for estimating ET rates, closely-related to those derived for the superexchange mechanism [1], specifically applied to ET by the McConnell expression [2], have found extensive application especially for biological systems [3, 4, 5] and they continue to be widely used for such systems (*e.g.* photosynthesis, proteins, DNA) [6, 7, 8, 9, 10, 11].

The Landauer formula states that the electronic conductance through a molecule connected to two leads is proportional to the transmission, a quantity which depends on the scattering processes involved. Some of the methods used to describe the scattering include Green's function methods, transfer matrix approaches [12], or the use of Lippmann-Schwinger scattering operators for mapping the non-equilibrium system onto an equilibrium one [13]. All of these methods are time-independent, thus enabling the use of the Landauer or, in the case of several leads, the Landauer-Büttiker formula, for evaluating the current.

Most studies of electron transmission through bridges, *e.g.* Ref. [14], are in fact based on non-equilibrium Green's function methods rather than explicitly time-dependent calculations. Recently however, time-dependent approaches are increasingly being applied. For instance the wave-packet dynamics

*Corresponding author
Email address: dpsiachos@gmail.com (D. Psiachos)

approach, wherein a spatially-Gaussian wavepacket with the Fermi energy of a scanning-tunnelling microscope tip bulk is launched towards the tip apex and tunnels into the sample [15]. Time-dependent approaches for studying the transfer of a wavepacket through organic molecules attached to electrodes [16] using Green’s function formalism have also been used in combination with perturbation theory to study the transfer in the presence of dissipation [17]. In such wavepacket approaches though, the transmission function is simply a Fourier-transform of the system (tip-sample or molecule+electrodes). This is to be contrasted with an explicit inclusion of the wavepacket as part of the system [18] where the eigenvalue spectrum can be modified by an incident electron off-resonance, leading to effects such as D-A tunnelling. Time-dependent forms of the transfer-matrix element owing to lattice effects were derived in Ref. [19] while a detailed comparison of the ET mechanisms identified the “through-bridge” contribution (‘sequential’ here) as a competing mechanism to that of the superexchange contribution [20] (‘direct’ ET here).

In all of the scattering methods described above, the standard implementation is that the scattered electron does not modify the existing energy level structure. Nonetheless, a vast body of literature exists where the influence of the transferred electron has been taken into account for calculating the Green’s function. In most cases, one desires only the projection onto a two-state approximation for D-A ET as a representation of the ‘direct’ ET occurring, even though, as shown later, this quantity does not in general capture all of the time-dependent phenomena. In a recent study [21], perturbation theory was compared with a self-consistent two-state construction based on the Löwdin projection [22]. Further back, an analytical, exact, expression for ET was derived for general bridge systems [23], similar to the work presented here for specific models. Numerically, the Green’s function for large systems has been calculated using non-perturbative techniques [24] and a procedure for an exact solution has been proposed [25]. Also, the approximations underlying the McConnell transfer-rate expression, have been assessed and various degrees of improvements proposed [26]. In line with the latter is the work by Stuchebrukhov (*e.g.* Ref. [27]) where the focus is on T-matrix expansions in order to achieve more accurate two-state pictures. However, the iterative techniques aimed at improving the accuracy of the Green’s function are confined to have certain regimes of validity, and fail near the resonant-transfer limit [28, 29, 30]. In addition, they are not general enough, in assuming equal donor and acceptor energies.

While an accurate calculation of the exact energy-level structure leads to improved rate expressions, at least for direct ET, for conductance calculations the scattering approach cannot be relied upon in cases where the ET is a transient phenomenon. In a series of papers [31, 32, 33] the current through small bridge molecules has been calculated time-dependently, in the presence of an electric field. Most notably, agreement was found with scattering theory in the steady-state regime [33], which nevertheless may be inapplicable to the small time scales of interest in ET in many cases. Recently, the Multi-configuration time-dependent Hartree method has been applied to study coherence in ultrafast electron

transfer, including electronic-vibrational coupling [34] while this method has been compared with a time-dependent Green's function method within a reduced density matrix formalism in Ref. [35] to span a wide range of time scales.

In this work, we correct the superexchange contribution at first instance, by deriving exact expressions for D-A ET for simple benchmark systems. We then elaborate using full time-dependent calculations of ET through the system attached to electrodes on the meaningfulness of the superexchange (what we refer to as “direct”) versus sequential ET as the energy of the transferred electron is varied. In our work, we do not aim to achieve the “steady-state” regime but we compare our results with the steady-state approaches, finding large differences. We further predict tunnelling-mediated increases in current transmission, which are completely inaccessible by the scattering model.

2. Theoretical Methods

We aim at an exact solution for ET in the D-B-A systems shown in Fig. 1, in the spirit of Ref. [23] who considered exact approaches for deriving two-state effective Hamiltonians for general D-B-A systems. They consist of a single bridge (Model A), two equivalent though non-interacting bridges (parallel configuration, Model B), and two oppositely-configured bridges (Model C). The bridge energy is offset in general by $|\epsilon_B|$ from the donor and acceptor energy levels, which have been made equal for simplicity. Movement of electrons between the bridges and the donor or acceptor levels is accomplished by a hopping energy t . In a later section (Sec. 4.1.2) we calculate the current transmission through the D-B-A system when attached to electrodes.

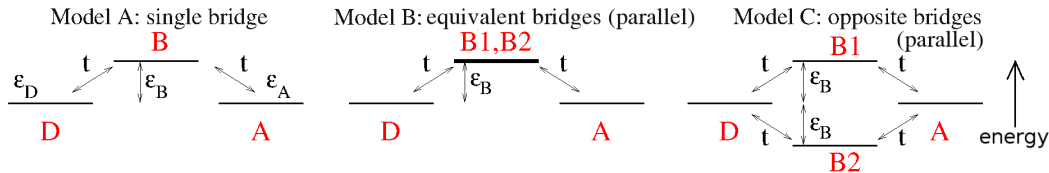


Figure 1: The three model Donor-Bridge-Acceptor (D-B-A) systems under study. The donor energy ϵ_D is depicted as equal to the acceptor energy ϵ_A for clarity.

The Hamiltonian in second-quantized form describing these systems is given by

$$H = \sum_{i,\sigma} \epsilon_i c_{i,\sigma}^\dagger c_{i,\sigma} - t \sum_{\langle i,j \rangle, \sigma} \left(c_{i,\sigma}^\dagger c_{j,\sigma} + c_{j,\sigma}^\dagger c_{i,\sigma} \right) \quad (1)$$

where $\langle i, j \rangle$ denotes that the hopping with energy t is restricted to nearest neighbours, while the ϵ_i term describes the on-site energy of the electron.

In the site basis ($|D\rangle, |A\rangle, |B\rangle$) (the order between B and A having been reversed to write it in block form), H for the system depicted in Model A of Fig. 1 is

$$H = \left(\begin{array}{cc|c} \epsilon_D & 0 & -t \\ 0 & \epsilon_A & -t \\ \hline -t & -t & E_B \end{array} \right) \quad (2)$$

where E_B is the bridge energy. Explicitly, in terms of the electron occupation on the three sites (D-B-A) of Model A, the basis is $|D\rangle \equiv |\uparrow, \cdot, \cdot\rangle$, $|B\rangle \equiv |\cdot, \uparrow, \cdot\rangle$, $|A\rangle \equiv |\cdot, \cdot, \uparrow\rangle$.

By itself, a diagonalization of Eq. 2 gives no information in general on the direct transfer from D to A. In contrast, for superexchange [36], a direct diagonalization yields the lowest singlet and triplet eigenstates, which are used to determine the superexchange interaction J . To study ET using Eq. 2, an electron needs to be set up at time $t = 0$ at site D , and its time evolution to A studied using the time-dependent Schrödinger equation (TDSE). Not in the least because the number of B sites could be extremely large, it is frequently preferred to extract approximate parameters for describing ET using effective Hamiltonians. Thus, we may use one of the well-known procedures for constructing an effective Hamiltonian between D and A and examine the off-diagonal, transfer-matrix element. In simple rate expressions *e.g.* Refs.[2, 4] the rate is proportional to the squared magnitude of the transfer-matrix element. In more sophisticated models the electron-nuclei interactions are treated in greater detail [19, 37, 38].

2.1. Effective Hamiltonian

The blocks of the Hamiltonian Eq. 2 are denoted by the following short-hand notation:

$$H = \left(\begin{array}{c|c} \underline{H_{00}} & \underline{T_{01}} \\ \hline \underline{T_{10}} & \underline{H_{11}} \end{array} \right). \quad (3)$$

The purpose of defining an effective Hamiltonian is to describe the full Hamiltonian in terms of a subset of the full basis, in this case the $\underline{H_{00}}$ block. An exact projection may be obtained from a Löwdin approach [22]. The solution, in terms of the notation of Eq. 3, is given by

$$H_{\text{eff}}(E) = \underline{H_{00}} + \underline{T_{01}} \left(E\underline{I} - \underline{H_{11}} \right)^{-1} \underline{T_{10}}. \quad (4)$$

Explicitly, and after making the system symmetric and redefining the energy zero for simplicity in comparing with literature results; $\epsilon_D = \epsilon_A \equiv 0$, Eq. 4 is given by

$$H_{\text{eff}}(E) = \left(\begin{array}{cc} \frac{t^2}{E - \epsilon_B} & \frac{t^2}{E - \epsilon_B} \\ \frac{t^2}{E - \epsilon_B} & \frac{t^2}{E - \epsilon_B} \end{array} \right), \quad (5)$$

while our eigenvalue problem is now

$$H_{\text{eff}}(E)X = EX, \quad X = (c_1 |D\rangle, c_2 |A\rangle), \quad (6)$$

that is the eigenvectors are a linear combination of D and A states.

The quantity E is the ET energy and it can be determined exactly. It can lead to the exact eigenvalue for *one* element at a time in X if it is set to the corresponding eigenvalue of Eq. 6. However, most of the time it is set to the unperturbed eigenvalue, in this case ϵ_D or ϵ_A , as per Rayleigh-Schrödinger perturbation theory [39, 40], with the aim of using one effective Hamiltonian for describing all solutions

within an energetically-degenerate subspace. In this work, we will show that this leads to qualitatively incorrect behaviour, while Model C is completely untreatable by perturbation theory.

By solving Eq. 6 three distinct roots, labelled $\lambda_1, \lambda_2, \lambda_3$, are obtained, exactly equal to the eigenvalues of the full H, Eq. 2, for all parameter values.

Fig. 2 shows the three roots as the bridge energy relative to the ends (which are set equal: $\epsilon_D = \epsilon_A$) is varied.

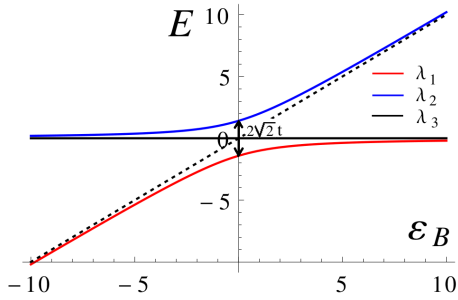


Figure 2: The three energy eigenvalues of Eq. 5 as the relative bridge energy is varied for $\epsilon_D = \epsilon_A$. The dashed line is an asymptote: $E = \epsilon_B$, shown as a guide to the eye. Scales in units of t .

3. D-A Effective Transfer

Here the results for the off-diagonal term of Eq. 5, hereafter denoted by T_{DA} , when E is replaced by the three exact eigenvalues (Fig. 2) are shown, again assuming the symmetric case $\epsilon_D = \epsilon_A \equiv 0$, although this method works for general parameters.

The elements in Eq. 5 are not in general second-order in t ; this is true only for $t/|\epsilon_B| \ll 1$ for the symmetric case studied here.

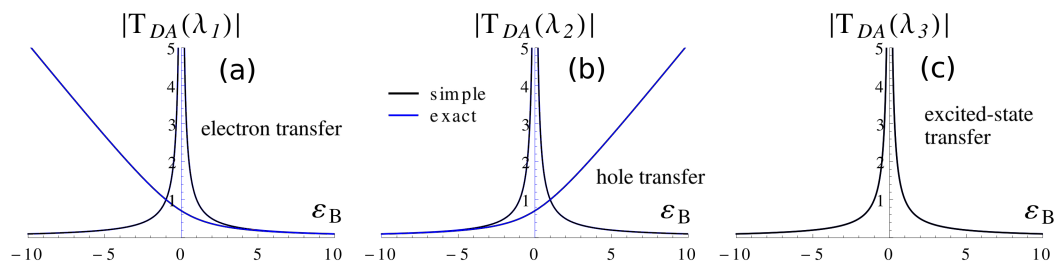


Figure 3: The effective transfer $|T_{DA}|$ according to the each of the eigenvalues (see Fig. 2) in two forms: the ‘simple’ and the exact form (see text). For λ_3 the two forms coincide. Scales in units of t .

In Fig. 3 there are two forms of the effective transfer shown: the ‘simple’ form from using the unperturbed D/A energies in Eq. 5 and the exact form. Fig. 3a depicts ET as it was derived using the lowest eigenvalue. Fig. 3b corresponds to hole transfer, which dominates when $\epsilon_B < 0$. For $\epsilon_B \neq 0$ we have contributions from both; depending on their relative signs, either electron or hole transfer dominates, while at resonance $\epsilon_B = 0$, the two contributions are equal.

Indeed, a full time-dependent analysis of D-A transfer from solving the TDSE shows that the transfer of a wavepacket originating on D contains three time-scales, or Rabi frequencies. The occupation probability at A may be written as

$$|\psi_A(t)|^2 = \sum_{i=1}^3 A_i \cos 2\omega_i t \quad (7)$$

where the ω_i are equal to $T_{DA}(\lambda_1)$ for ET, to $T_{DA}(\lambda_2)$ for hole transfer, or to the sum of the two. None of the Rabi frequencies ω_i however is equal to $T_{DA}(\lambda_3)$, which corresponds to excited-state transfer of a wavepacket.

As well, the functions $T_{DA}(\lambda_1)$ and $T_{DA}(\lambda_2)$ are finite-valued at $\epsilon_B = 0$ unlike the expression $T_{DA}(\lambda_3)$ (Fig. 3). In Fig. 3 the exact and ‘simple’ expressions coincide, although λ_3 is not the lowest eigenvalue. λ_3 is degenerate with one of the other two roots for large $|\epsilon_B|$ only and therefore the results of T_{DA} derived using this root are invalid at smaller $|\epsilon_B|$. Specifically, when $\epsilon_B = 0$ the exact results for T_{DA} are $t/\sqrt{2}$, $-t/\sqrt{2}$, and ∞ for the three roots λ_1 , λ_2 , and λ_3 respectively.

These results generalize for a bridge composed of many sequential sites.

3.1. Independent paths

Without loss of generality, we consider two independent paths from D-A, seen for example in Fig. 1 Models B,C. We again treat the donor and acceptor energy levels as equal for simplicity. However, the two bridges may be non-equivalent. We take the extreme cases where the two bridges have the same energy, or where one energy is the negative of the other. Such situations would arise from considering bonding or anti-bonding configurations of π orbitals or more complex molecules [41]. Such general forms of bridge structures and the consideration of independent pathways are, for example, applicable to proteins and to photosynthesis molecules [8, 9, 11].

The Hamiltonian is written, again assuming $\epsilon_D = \epsilon_A \equiv 0$ as

$$H = \left(\begin{array}{cc|cc} 0 & 0 & -t & -t \\ 0 & 0 & -t & -t \\ \hline -t & -t & \epsilon_{B1} & 0 \\ -t & -t & 0 & \epsilon_{B2} \end{array} \right) \begin{array}{l} |\uparrow, \cdot, \cdot, \cdot\rangle \equiv |D\rangle \\ |\cdot, \cdot, \cdot, \uparrow\rangle \equiv |A\rangle \\ |\cdot, \uparrow, \cdot, \cdot\rangle \equiv |B1\rangle \\ |\cdot, \cdot, \uparrow, \cdot\rangle \equiv |B2\rangle \end{array} \quad (8)$$

while the result of the projection onto the model space ($|D\rangle$, $|A\rangle$) is

$$H_{\text{eff}}(E) = \left(\begin{array}{cc} \frac{2t^2}{E-\epsilon_B} & \frac{2t^2}{E-\epsilon_B} \\ \frac{2t^2}{E-\epsilon_B} & \frac{2t^2}{E-\epsilon_B} \end{array} \right) \begin{array}{l} |D\rangle \\ |A\rangle \end{array} \quad (9)$$

for equivalent bridge levels $\epsilon_{B1} = \epsilon_{B2} \equiv \epsilon_B$ and

$$H_{\text{eff}}(E) = \left(\begin{array}{cc} \frac{2Et^2}{E^2-\epsilon_B^2} & \frac{2Et^2}{E^2-\epsilon_B^2} \\ \frac{2Et^2}{E^2-\epsilon_B^2} & \frac{2Et^2}{E^2-\epsilon_B^2} \end{array} \right) \begin{array}{l} |D\rangle \\ |A\rangle \end{array} \quad (10)$$

for opposite bridge levels, $\epsilon_{B1} = -\epsilon_{B2} \equiv \epsilon_B$ (Fig. 1).

In the first case, of equivalent bridges (Model B), the results are quite similar to the single-bridge case. The eigenvalues of Eq. 9 and the corresponding transfer element for the lowest root are shown in

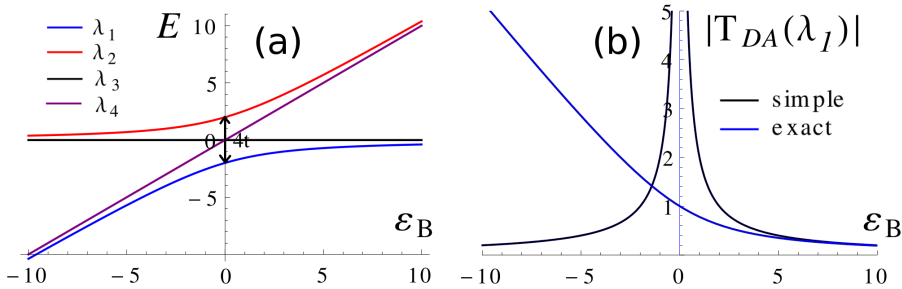


Figure 4: (a) The eigenvalues of the equivalent-bridge situation (Eq. 9) as a function of the bridge energy. (b) The effective transfer $|T_{DA}|$ according to the lowest eigenvalue of the equivalent-bridge case in the ‘simple’ as well as the exact form (see text). $\epsilon_D = \epsilon_A = 0$ has been assumed. The energy scales are in terms of t .

Figs. 4a and b where again the ‘simple’ expression obtained using the unperturbed D/A energies in Eq. 9 is included for comparison.

As in the single-bridge case, the transfer element only asymptotically approaches the ‘simple’ expression, where the unknown energy E in Eq. 9 was set equal to the unperturbed energy $\epsilon_D = \epsilon_A = 0$. In the ‘simple’ form, the transfer element for the two independent bridges is twice that of the single bridge: $\left| \frac{2t^2}{\epsilon_B} \right|$, but this is not the case when the exact expressions for E are used.

In the case of bridge energy levels having opposite signs (Model C), we get the eigenvalues and transfer elements of Fig. 5. Clearly, there is no asymptotic approach of the upper/lower eigenvalues to any of the

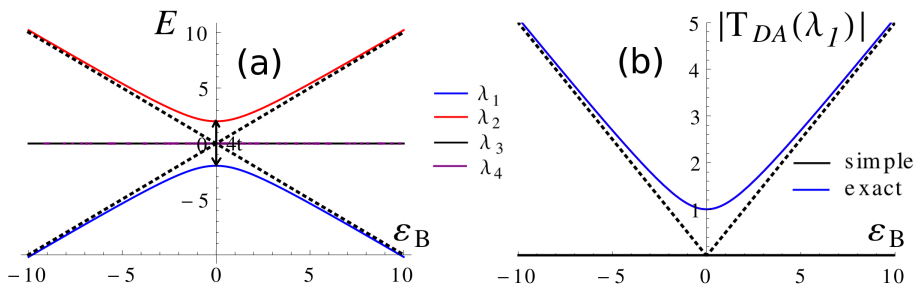


Figure 5: The eigenvalues and corresponding transfer parameters for the opposite-bridge case where $\epsilon_D = \epsilon_A = 0$ has been assumed. The eigenvalues λ_3 and λ_4 in (a) are always zero. Similarly, the ‘simple’ expression in (b) is zero. Dashed lines correspond to the asymptotes $E = \pm \mathcal{E}_B$ and $|T_{DA}| = \pm \frac{1}{2} \mathcal{E}_B$ which are guides to the eye. Scales in terms of t .

other roots. The use of the unperturbed energy results in destructive interference, or $T_{DA} = 0$, as can be seen by Eq. 10 but this value is never accessed, except perhaps in an excited-state form of transfer.

4. Transmission Characteristics

The significance of the transfer matrix element is that it approximates ET by a single Rabi frequency, which is exactly the dominant Rabi frequency of the time-dependent solution of the full H. However, it tells us nothing about the amplitude of the transfer. In Fig. 5 the transfer element gets *larger* as the bridge energies move off resonance, meaning that in the simplest of models [2, 4] the transfer rate is

increased. However, the actual amplitude of this dominant contribution to the ET (the coefficient A_i of this term in Eq. 7) is vastly reduced, with the consequence that the rate of ET is reduced.

This is why quantities such as, the wavepacket transmission and the current transmission for the D/A system attached to electrodes are more meaningful. Notably, the current combines both qualities: rate and amplitude while the conductance measured in experiments is proportional to transmission.

The D-B-A system coupled to electrodes was set up as in Fig 6. At time zero, The transferred electron is imparted with an energy E on a site at the far end of the left electrode while the wavepacket amplitude or current is calculated at a reference point located deep inside the electrode in order to avoid the effects of reflection from the bridge. The location of the transmission probe had no effect. The effect of the electrodes is minimal when the coupling to the D-B-A system (hopping ν) is small compared with the hopping t_0 in the wires.

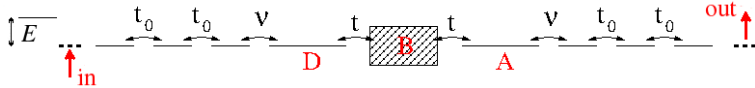


Figure 6: The D-B-A system attached via a coupling ν to tight-binding electrodes with electron hopping t_0 . An energy E is imparted to the transferred electron at the far-left. Shown are the locations, deep inside the electrodes, where the incoming and outgoing quantities are probed.

The evolution of the wavefunction, using the TDSE, was performed using finite electrodes, each numbering 500 sites, longer than necessary for the results to converge. While using lattice Green's functions, the length of the electrodes can in principle be extended to infinity, the ranges must nonetheless be truncated in space if the interaction is to be maintained in its exact form. By using finite electrodes it is a simple matter to impart an energy E to the transferring electron at the left-most site, as seen in Fig. 6. As it is localized on a non-eigenstate, it transfers even with no external field present. During the time evolution, the total energy of the system is conserved as is that of each electronic wavefunction separately since the electrons are non-interacting.

4.1. Scattering-based versus time-dependent energy spectrum

We compare our time-dependent calculation with that of a Fourier-transformed energy spectrum (scattering method) in which the transmission is computed in terms of the scattered electron energy. In contrast, for the exact-diagonalization approach, the expectation value of the energy is referred to since the energy of the extra electron does not correspond to an eigenvalue of the system. The Fourier-transform calculation of the transmission additionally differs from the explicit inclusion of the transferred electron as in the 'simple' calculation of T_{DA} : they are both lowest-order perturbation calculations. Thus the comparison will have both of these differences. However, for long bridges it is expected that the difference arising from the use of the expectation value versus the exact energy will be minimal. We calculate both the wavepacket and the current transmission, comparing the time-dependent results with scattering theory.

4.1.1. Wavepacket Transmission

In Fig. 7 we show the transmission of the probability density for a variety of molecule configurations as a function of scattering energy E . The following geometries were studied: a single molecule, and two molecules in the parallel-path configuration oriented either with the same or opposite energies, as in Fig. 1. In the exact approach the energy-dependent probability density is obtained by integrating the strongly-peaked wavepacket over a window: $\left| \int \psi_{extra}(E, t) dt \right|^2$ while in the scattering approach it is expressed as a Fourier-Transform: $\left| \tilde{\psi}_{extra}(E) \right|^2$.

In the scattering approach, the height and location of the peaks in the transmission in Fig. 7a are determined by the bridge-molecule characteristics: energy of the bridge as well its coupling to the electrodes. The latter is kept small in order to minimize the effect of the electrodes. The effect of two parallel bridges is to increase the transmission of the scattered electron at $E = 0$ when the bridge-molecule energy is different from that of the wires; the larger the bridge-molecule energy is the closer the transmission gets to achieving a doubling of its value in the single bridge case. For oppositely-configured bridges the transmission is zero at $E = 0$ (anti-resonance). However, at non-zero E , the transmission can be enhanced compared to the single-bridge case. Generally, the double bridges lead to enhanced transmission over a wide range of scattering energies of the electron. The results compare well with the existing literature [42, 43, 17] while the band edge at $\pm 2t_0$ becomes a sharp cutoff in the transmission as the length of the electrodes approaches infinity (not shown).

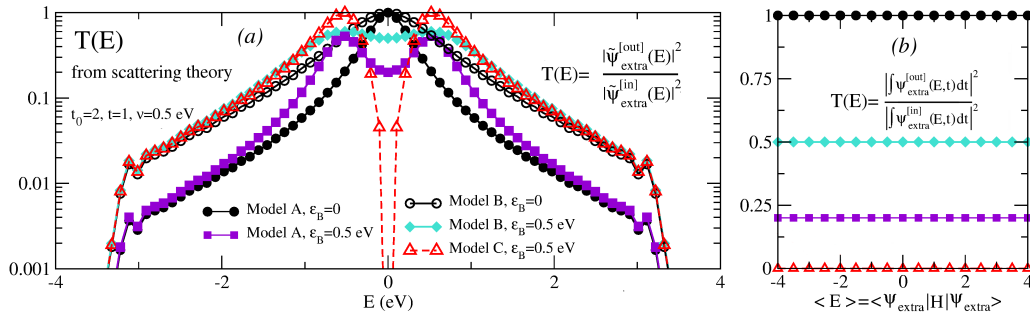


Figure 7: Transmission of electron probability density across the bridge for various bridge-molecule configurations as indicated in the legend (see also Fig. 1) as a function of the electron-scattering energy E (a) or its expectation value $\langle E \rangle$ (b). Diagram (a): using scattering theory (Fourier-Transform), indicated by the tilde ($\tilde{}$) sign. Diagram (b): with exact diagonalization. The results for Model A and Model B at $\epsilon_B = 0$ coincide. The input/output values were taken at 100 electrode sites before/after the bridge (schematic in Fig. 6).

For the explicitly time-dependent calculations, the results are completely different, as can be seen in Fig. 7b, the two agreeing only at zero electron energy. Rather than displaying resonances and anti-resonances, the spectrum is completely flat, as would be expected from the frequency response to an impulse input. Rather than being dominated by the structure of the D-B-A system, the frequency response is determined by the transferred electron, with the D-B-A system imparting only a constant modification. The destructive interference in model C in particular holds for all energies. The effect of parallel, equivalent bridges (model B) off resonance is to more than double the transmission compared

to a single bridge (model A), an effect previously found in conductance experiments [41, 44]. One study found that electronic effects (functional groups) do not greatly modify single-molecule conductance [45] while geometrical (conformation) effects do have some effect [46].

4.1.2. Current Transmission

As the wavepacket transmission is not normally observed in experiments, we choose to study the current transmission. The continuous-current formula

$$\frac{\partial \rho}{\partial t} + \nabla \cdot \vec{j} = 0 \quad (11)$$

has the discretized form at the link between the n th and the $n + 1$ th sites (separated by the lattice spacing a) of a tight-binding chain [47]

$$j_{n,n+1} = \frac{i}{\hbar} a t_0 (\psi_{n+1}^* \psi_n - \psi_n^* \psi_{n+1}) \quad (12)$$

whence the current at the energy E is given by

$$J(E) = \int_{t=0}^{\infty} j(E, t) dt. \quad (13)$$

The current is found to be very strongly-peaked and Eq. 13 is thus integrated over a window so as not to be influenced by reflection from the wire ends. Although some authors [16] consider that Eq. 13 describes the transmission $T(E)$ directly, we label it as $J(E)$ as in our case we calculate the transmission with respect to a point deep inside the left electrode (Fig. 6) and we thus need to normalize it in terms of that quantity.

We compare the current according to Eq.13 for the exact, time-dependent case (with the expectation value of the energy) with the Fourier-transformed current, which is appropriate for a steady-state situation, in Fig. 8. As in the case of the wavepacket transmission, the results agree only at zero energy. What is most striking in the comparison of the results obtained using the two methods is that while both begin by dropping off overall for increasing energy, in the exact approach, the current transmission *increases* at

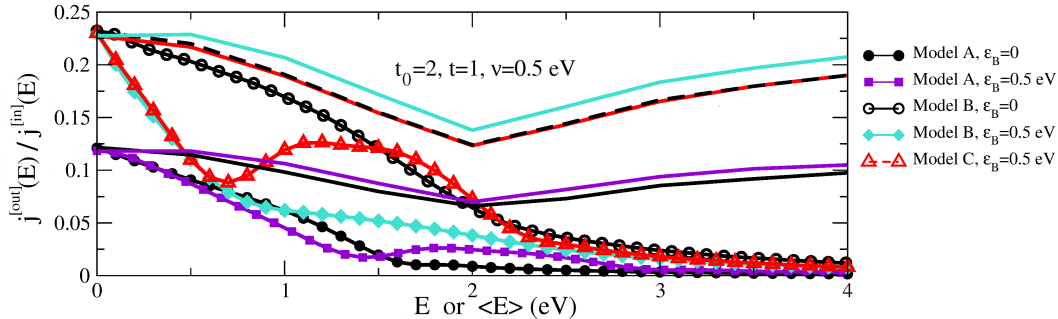


Figure 8: Transmission of current across the bridge for various bridge-molecule configurations as a function of energy E . The coupling parameter of the electrode to the bridge is $\nu = 0.5$. Compared are the scattering (symbols) and the exact (bare lines) approaches. Otherwise the colour correspondence shown in the legend applies to both approaches, only that the bare dashed black line (exact approach) corresponds to the case of Model B, $\epsilon_B = 0$ (open circle in scattering approach).

higher energies ($E > t_0$) and levels off. The reduction in the current transmission with increasing E (up to t_0 , that is 2 eV) is due to two factors: off-resonant transmission in which the transmitted wavepacket increasingly prefers to occupy lower density-of-states regions at the edges of the bands, which are shaped as such on account of the defect D-B-A system, and secondly due to the back-reflection of incoming and pinning of outgoing electrons at the D-B-A system owing to the small coupling to electrodes ν compared with the other hopping parameters. The latter is the cause of the current transmission being small even at $E = 0$. Note that in this regard there is a substantive difference with Fig. 7a which does reach values of 1. The quantity $\frac{\int |\psi_{\text{extra}}^{[\text{out}]}(E,t)|^2 dt}{\int |\psi_{\text{extra}}^{[\text{in}]}(E,t)|^2 dt}$, termed the *occupation transmission*, resembles the ‘exact’ curves in Fig. 8 qualitatively and quantitatively (not shown).

At values of $E < t_0$ the current transmission occurs via a ‘sequential’ mechanism in which each site is distinctly occupied in sequence but at $E > t_0$ the main mode of transmission is via a tunnelling mechanism via a defect state which splits off above the conduction-band maximum which becomes increasingly favoured for higher E . Because we are also in the direct ET regime in which the D-B-A system is now practically unoccupied, there is much less loss of transmission due to pinning or back-reflection, leading to the increase in current transmission. At $E = 0$ the current transmission for the parallel bridge configurations (models B and C) is double that of model A while there is no destructive interference for model C.

5. Conclusions

We have calculated the exact electron-transfer (ET) matrix elements for a few benchmark donor-bridge-acceptor systems and we have found them to differ remarkably from the results obtained from perturbation theory. Rayleigh-Schrödinger perturbation theory does not in general lead, at any order, to the exact results. Regardless, ET rates, which depend on the dominant Rabi frequency of the transfer from donor to acceptor, are not representative of experimental measurements of more relevant quantities such as current or wavepacket transmission / conductance. For our models, we find, in agreement with some experiments, that current transmission is actually not very sensitive to the bridge geometry but more to the number of parallel pathways. In the wavepacket transmission we do however find destructive interference for one of the bridge configurations, but for all energies. In the current transmission we find constructive but no destructive interferences resulting from the bridge-model geometries we studied. For the wavepacket transmission we find a flat transmission spectrum in the exact approach involving the explicit inclusion of the transferred electron as an impulse, in contrast with the time-independent, scattering approach, which is appropriate to steady-state situations. The current transmission further displays an unexpected characteristic for large energies: it increases as a result of tunnelling involving defect states split off from the conduction-band maximum, an effect not captured by scattering theory where the existing energy levels are not altered by the impinging electron.

[1] P. W. Anderson. *Physical Review*, 79:350, 1950.

- [2] H. M. McConnell. *J. Chem. Phys.*, 35:508, 1961.
- [3] R. Haberkorn, M. E. Michel-Beyerle, and R. A. Marcus. *Proc. Natl. Acad. Sci. USA*, 76:4185, 1979.
- [4] R. A. Marcus. *Chem. Phys. Lett.*, 133:471, 1986.
- [5] A. Ogrodnik, N. Remy-Richter, and M. E. Michel-Beyerle. *Chem. Phys. Lett.*, 135:576, 1987.
- [6] S. S. Skourtis, D. H. Waldeck, and D. N. Beratan. *J. Phys. Chem. B*, 1108:15511, 2004.
- [7] M. L. Kirk, D. A. Shultz, E. C. Depperman, and C. L. Brannen. *J. Am. Chem. Soc.*, 129:1937, 2007.
- [8] M. A. Ratner. *J. Phys. Chem.*, 94:4877, 1990.
- [9] D. N. Beratan, S. S. Skourtis, I. A. Balabin, A. Balaeff, S. Keinan, R. Venkatramani, and D. Xiao. *Acc. Chem. Res.*, 42:1669, 2009.
- [10] D. Xiao, S. S. Skourtis, I. V. Rubtsov, and D. N. Beratan. *Nano. Lett.*, 9:1818, 2009.
- [11] M. Zarea, D. Powell, N. Renaud, M. Wasielewski, and M. A. Ratner. *J. Phys. Chem. B*, 117:1010, 2013.
- [12] P. Sautet and C. Joachim. *Phys. Rev. B*, 38:12238–12247, 1988.
- [13] J. E. Han. *Phys. Rev. B*, 73:125319–1–9, 2006.
- [14] T. Frederiksen, M. Paulsson, M. Brandbyge, and A.-P. Jauho. *Phys. Rev. B*, 75:205413–1–22, 2007.
- [15] G. I. Márk, P. Vancsó, C. Hwang, P. Lambin, and L. P. Biró. *Phys. Rev. B*, 85:125443, 2012.
- [16] Z. G. Yu, D. L. Smith, A. Saxena, and A. R. Bishop. *Phys. Rev. B*, 59:16001–16010, 1999.
- [17] N. Renaud, M. Ratner, and C. Joachim. *J. Phys. Chem. B*, 115:5582–5592, 2011.
- [18] D. Psiachos. *Chem. Phys.*, 436-437:8, 2014.
- [19] Q. Xie, G. Archontis, and S. S. Skourtis. *Chem. Phys. Lett.*, 312:237, 1999.
- [20] S. S. Skourtis, G. Archontis, and Q. Xie. *J. Chem. Phys.*, 115:9444, 2001.
- [21] H. Nishioka and K. Ando. *Phys. Chem. Chem. Phys.*, 13:7043–7059, 2011.
- [22] P.O. Löwdin. *J. Math. Phys.*, 3:969, 1962.
- [23] J. W. Evenson and M. Karplus. *J. Chem. Phys.*, 96:5272, 1992.
- [24] A. Okada, T. Kakitani, and J. Inoue. *J. Phys. Chem.*, 99:2946, 1995.

- [25] J. N. Onuchic, P. C. P. de Andrade, and D. N. Beratan. *J. Chem. Phys.*, 95:1131, 1991.
- [26] J. R. Reimers and N. S. Hush. *J. Photochem. Photobiol. A: Chem.*, 82:31, 1994.
- [27] A. A. Stuchebrukhov. *Chem. Phys. Lett.*, 265:643, 1997.
- [28] S. S. Skourtis and J. N. Onuchic. *Chem. Phys. Lett.*, 209:171, 1993.
- [29] S. S. Skourtis, D. N. Beratan, and J. N. Onuchic. *Chem. Phys.*, 176:501, 1993.
- [30] S. Priyadarshy, S. S. Skourtis, S. M. Risser, and D. N. Beratan. *J. Chem. Phys.*, 104:9473, 1996.
- [31] A. T. Amos and B. L. Burrows. *Int. J. Quant. Chem.*, 74:585, 1999.
- [32] B. L. Burrows and A. T. Amos. *Int. J. Quant. Chem.*, 87:69, 2002.
- [33] B. L. Burrows and A. T. Amos. *Int. J. Quant. Chem.*, 107:1954, 2007.
- [34] J. Li, I. Kondov, H. Wang, and M. Thoss. *J. Phys.: Condens. Matter*, 27:6134202, 2015.
- [35] E. Y. Wilner, H. Wang, M. Thoss, and E. Rabani. *Phys. Rev. B*, 89:205129, 2014.
- [36] D. Psiachos. *Ann. Phys.*, 360:33–43, 2015.
- [37] H. Sumi and T. Kakitani. *J. Phys. Chem. B*, 105:9603, 2001.
- [38] J. Blumberger. *Chem. Rev.*, 115:11191, 2015.
- [39] I. Lindgren. *J. Phys. B: Atom. Molec. Phys.*, 7:2441, 1974.
- [40] I. Hubač and S. Wilson. *Brillouin-Wigner methods for many-body systems*, chapter 4. Springer, Dordrecht, 2010.
- [41] H. Vazquez, R. Skouta, S. Schneebeil, M. Kamenetska, R. Breslow, L. Venkataraman, and M. S. Hybertsen. *Nature Nanotech.*, 7:663, 2012.
- [42] B. T. Pickup and P. W. Fowler. *Chem. Phys. Lett.*, 459:198, 2008.
- [43] G. C. Solomon, D. Q. Andrews, T. Hansen, R. H. Goldsmith, M. R. Wasielewski, R. P. Van Duyne, and M. A. Ratner. *J. Chem. Phys.*, 129:054701, 2008.
- [44] M. Kiguchi, Y. Takahashi, S. Fujii, M. Takase, T. Narita, M. Iyoda, M. Horikawa, Y. Naitoh, and H. Nakamura. *J. Phys. Chem. C*, 118:5275, 2014.
- [45] D. J. Mowbray, G. Jones, and K. S. Thygesen. *J. Chem. Phys.*, 128:111103, 2008.
- [46] L. Venkataraman, J. E. Klare, C. Nuckolls, M. S. Hybertsen, and M. L. Steigerwald. *Nature*, 442:904, 2006.
- [47] T. B. Boykin, M. Luisier, and G. Klimeck. *Eur. J. Phys.*, 31:1077, 2010.